

Warm target recoil ion momentum spectroscopy for fragmentation of molecular hydrogen by ultrashort laser pulses

Jia Liu¹, Jian Wu¹, Achim Czasch², and Heping Zeng¹

¹State Key Laboratory of Precision Spectroscopy, East China Normal University, Shanghai 200062, China

²Institut für Kernphysik Frankfurt D-60438, Frankfurt am Main, Germany

jwu@phy.ecnu.edu.cn, hpzeng@phy.ecnu.edu.cn

Abstract: We demonstrate warm target recoil ion momentum spectroscopy for the fragmentation dynamics of the warm hydrogen molecules at room temperature. The thermal movement effect of the warm molecule is removed by using a correction algorithm in the momentum space. Based on the reconstructed three-dimensional momentum vectors as well as the kinetic energy release spectra, different vibrational states of the H_2^+ ground state are clearly visible and the internuclear separation for charge resonance enhanced ionization of the second electron is identified. The results show adequate accordance with the former experiments using other techniques.

©2009 Optical Society of America

OCIS codes: (020.2649) Strong field laser physics; (020.4180) Multiphoton processes

References and links

1. R. Dörner, V. Mergel, O. Jagutzki, L. Spielberger, J. Ullrich, R. Moshhammer, H. Schmidt-Böcking, "Cold Target Recoil Ion Momentum Spectroscopy: a 'momentum microscope' to view atomic collision dynamics," *Phys. Rep.* **330**, 95-192 (2000).
2. E. Gagnon, A.S. Sandhu, A. Paul, K. Hagen, A. Czasch, T. Jahnke, P. Ranitovic, C.L. Cocke, B. Walker, M.M. Murnane, and H.C. Kapteyn, "Time-resolved momentum imaging system for molecular dynamics studies using a tabletop ultrafast extreme-ultraviolet light source," *Rev. Sci. Instrum.* **79**, 063102 (2008).
3. Th. Weber, M. Weckenbrock, A. Staudte, L. Spielberger, O. Jagutzki, V. Mergel, F. Afaneh, G. Urbasch, M. Vollmer, H. Giessen, and R. Dörner, "Recoil-Ion Momentum Distributions for Single and Double Ionization of Helium in Strong Laser Fields," *Phys. Rev. Lett.*, **84**, 443-446 (2000).
4. S. Alnaser, T. Osipov, E. P. Benis, A. Wech, B. Shan, C.L. Cocke, X.M. Tong and C. D. Lin, "Rescattering Double Ionization of D_2 and H_2 by Intense Laser Pulses," *Phys. Rev. Lett.* **91**, 163002 (2003).
5. B. D. Esry, A. M. Saylor, P. Q. Wang, K. D. Carnes, and I. Ben-Itzhak, "Above Threshold Coulomb Explosion of Molecules in Intense Laser Pulses," *Phys. Rev. Lett.* **97**, 013003 (2006).
6. Ben-Itzhak, P. Q. Wang, A. M. Saylor, K. D. Carnes, M. Leonard, B. D. Esry, A. S. Alnaser, B. Ulrich, X. M. Tong, I. V. Litvinyuk, C. M. Maharjan, P. Ranitovic, T. Osipov, S. Ghimire, Z. Chang, and C. L. Cocke, "Elusive enhanced ionization structure for H_2^+ in intense ultrashort laser pulses," *Phys. Rev. A* **78**, 063419 (2008).
7. P. H. Bucksbaum, A. Zavriyev, H. G. Muller, and D. W. Schumacher, "Softening of the H_2^+ molecular bond in intense laser fields," *Phys. Rev. Lett.* **64**, 1883-1886 (1990).
8. T. Seideman, M. Y. Ivanov, and P. B. Corkum, "Role of Electron Localization in Intense-Field Molecular Ionization," *Phys. Rev. Lett.* **75**, 2819-2822 (1995).
9. T. Zuo and A. D. Bandrauk, "Charge-resonance-enhanced ionization of diatomic molecular ions by intense lasers," *Phys. Rev. A* **52**, R2511-R2514 (1995).
10. S. Alnaser, X. M. Tong, T. Osipov, S. Voss, C. M. Maharjan, P. Ranitovic, B. Ulrich, B. Shan, Z. Chang, C. D. Lin, and C. L. Cocke, "Routes to Control of H_2 Coulomb Explosion in Few-Cycle Laser Pulses," *Phys. Rev. Lett.* **93**, 183202 (2004).
11. G. N. Gibson, M. Li, C. Guo, and J. Neira, "Strong-Field Dissociation and Ionization of H_2^+ using Ultrashort Laser Pulses," *Phys. Rev. Lett.* **79**, 2022-2025 (1997).
12. Rudenko, B. Feuerstein, K. Zrost, V. L. B. de Jesus, T. Ergler, C. Dimopoulou, C. D. Schröter, R. Moshhammer and J. Ullrich, "Fragmentation dynamics of molecular hydrogen in strong ultrashort laser pulses," *J. Phys. B: At. Mol. Opt. Phys.* **38**, 487-501 (2005).

13. Staudte, C. L. Cocke, M. H. Prior, A. Belkacem, C. Ray, H. W. Chong, T. E. Glover, R. W. Schoenlein, and U. Saalman, "Observation of a nearly isotropic, high-energy Coulomb explosion group in the fragmentation of D₂ by short laser pulses," *Phys. Rev. A* **65**, 020703 (2002).
 14. M. R. Thompson, M. K. Thomas, P. F. Taday, J. H. Posthumus, A. J. Langley, L. J. Frasinski and K. Codling, "One and two-color studies of the dissociative ionization and Coulomb explosion of H₂ with intense Ti:sapphire laser pulses," *J. Phys. B: At. Mol. Opt. Phys* **30** 5755-5772 (1997).
 15. L. J. Frasinski, K. Codling, and P. A. Hatherly, "Covariance Mapping: A Correlation Method Applied to Multiphoton Multiple Ionization," *Science* **246**, 1029-1031 (1989).
 16. P. Hering and C. Comaggia, "Coulomb explosion of N₂ and CO₂ using linearly and circularly polarized femtosecond laser pulses," *Phys. Rev. A* **59**, 2836-2843 (1999).
 17. J. Wu, H. Zeng, and C. Guo, "Polarization effects on nonsequential double ionization of molecular fragments in strong laser fields," *Phys. Rev. A* **75**, 043402 (2007).
 18. J. Wu, H. Zeng, and C. Guo, "Vertical and nonvertical transitions in triple-ionization-induced dissociation of diatomic molecules," *Phys. Rev. A* **74**, 065403 (2006).
 19. T. D. G. Walsh, F. A. Ilkov and S. L. Chin, "The dynamical behavior of H₂ and D₂ in a strong, femtosecond, titanium:sapphire laser field," *J Phys. B: At. Mol. Opt. Phys.* **30**, 2167-2175 (1997).
-

1. Introduction

The Coltrims (Cold target recoil ion momentum spectroscopy), with a distinct multi-hits imaging ability and high momentum resolution, is widely used in the research of momentum imaging of electron and ion dynamics in strong laser fields [1-3]. In general, ultracold target gas (~several mK) from supersonic jet expansion is used to rule out the thermal effects and obtain an optimal momentum resolution, which is actually difficult to handle. Here, we demonstrate the 3D momentum spectroscopy applicable on a room-temperature gas. We call this Wartrims (Warm target recoil ion momentum spectroscopy) as an allusion to Coltrims. It is shown that measurements of reactions where all fragments are charged do not necessarily need a supersonic gas jet system if a well-suited correction algorithm is applied on the data on an event-by-event basis. In this paper, as an example, we focus on the fragmentation dynamics of the molecular H₂ exposed to intense near-IR femtosecond laser pulses. Different fragmentation channels produce distinct features in the kinetic energy release spectrum [4-6], and different vibrational states are thus clearly visible. The results show an adequate accordance with the former experiments using cold targets.

2. Experimental setup

A schematic of the experimental setup is shown in Fig. 1(a). The femtosecond laser pulses from an amplified Ti:Sapphire laser system (800 nm, 40 fs, 1 kHz) were focused into an ultrahigh vacuum chamber (background pressure $\sim 10^{-10}$ Torr) by a $f=25$ cm lens. Rather than using a supersonic gas jet for Coltrims, the room-temperature target gas was introduced into the chamber through a variable leak valve. The photon-ionization-induced ions were detected by the multichannel plate at the end of the time-of-flight spectrometer. The position information was then extracted by the time difference of the signals at the ends of the delay line detector. The complete 3D momentum vectors of the fragments were eventually obtained by combining the time-of-flight spectra and position information.

3. Software cooling

Different ionization/dissociation channels are identified on the basis of their characteristic momentum distributions, and the rule of momentum conservation is applied to identify the true coincident channels, such as H₂ → H⁺+H⁺ for H₂. Similar to the Coltrims, here, the z-axis velocities of the ionic fragments are calculated based on the arriving time difference between the forward and backward ions, and the x-axis and y-axis velocities are deduced from the spatial distributions of the fragments on the detector. The obtained momentum vectors are then used to calculate the kinetic energy release and angular distributions of the ions. However, in our case with room temperature gas, before the molecule is destroyed it has a certain

velocity. Usually the thermal velocity is several hundred meters per second, corresponding to a kinetic energy of ~40 meV. Once the molecule is fragmented, the two ions fly away back to back from each other and land on the detector. Since each particle is measured independently from the other, it is possible to calculate the velocity of their center of mass, which can be subtracted from the two measured velocities. We then can obtain the momentum vectors as if the target gas is frozen. We call this technique as software cooling.

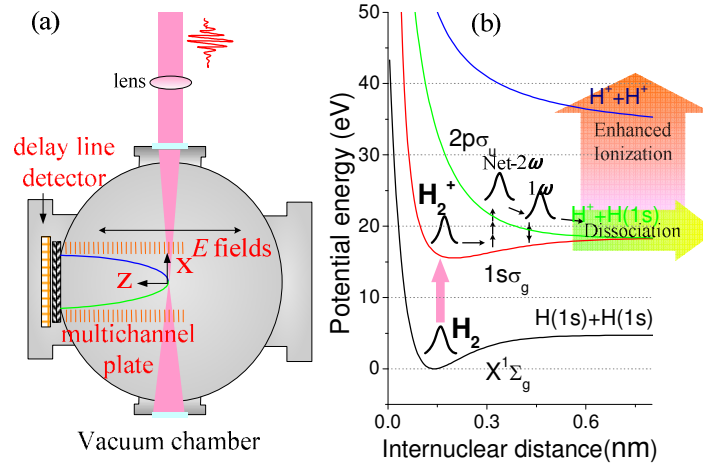


Fig. 1. (a) Schematic of the experimental apparatus. (b) Potential energy curves for H_2 and H_2^+ .

We take the Coulomb explosion of H_2 with an initial thermal velocity vector of $v_{thermo}=(1133.0, 1133.0, 1133.0) m/s$ as an example, the corresponding molecular kinetic energy and momentum vector are 40 meV and 0.944 a.u., respectively. Supposing that the kinetic energy each ion gains is 3.0 eV, and the molecule is oriented along the z-axis, the velocity of each H^+ fragments gain is 24063.2 m/s. Equation 1 shows the velocity vectors of the fragments

$$\begin{aligned} v_1 &= (1133.0, 1133.0, 24063.2 + 1133.0) m/s \\ v_2 &= (1133.0, 1133.0, -24063.2 + 1133.0) m/s \end{aligned} \quad (1)$$

This net kinetic energy gain of 3.0 eV can then be extracted from the measured signals by applying the software cooling conditions as

$$\begin{aligned} v_1' &= v_1 - (v_1 + v_2) / 2 = (v_1 - v_2) / 2 = (0, 0, 24063.2) m/s \\ v_2' &= v_2 - (v_1 + v_2) / 2 = (v_2 - v_1) / 2 = (0, 0, -24063.2) m/s \end{aligned} \quad (2)$$

which account for the real momenta or kinetic energy gain of the ionic fragments from the Coulomb explosion process. As shown in Eq. 2, the thermal effect of the warm target gas is removed, making our Wartrims a powerful tool for momentum analysis.

4. Results and discussions

H_2 has relatively simple ionization and breakup (H_2^{2+} , $H^+ + H^+$, H_2^+ , $H^+ + H$) channels as compared to other molecules. Figure 1(b) shows the potential energy curves of H_2 and H_2^+ . By single ionization of H_2 , the molecule (initially in the ground state) is excited to the $1s\sigma_g$ electronic state of molecular ion H_2^+ . The wave packets will propagate along this new potential curve, and the decrease of the energy gap between the ground $1s\sigma_g$ and the excited $2p\sigma_u$ states leads to subsequent breakup processes. Bond softening dissociation [7] (if more than the minimum number of photons are absorbed, it turns to the above-threshold

dissociation) and charge resonance enhanced ionization [8] are considered as the two main fragmentation channels. The charge resonance enhanced ionization results in an enhancement of the ionization rate at a critical internuclear distance R_c due to the barrier suppression at the specific internuclear separation [9], where a second electron is ionized and subsequently exploded into two H^+ [10]. In different H_2 experiments, the charge resonance enhanced ionization, which gives the largest ionization probability in the kinetic energy release of 2-4 eV, is observed and considered as the dominant channel of sequential ionization [11,12].

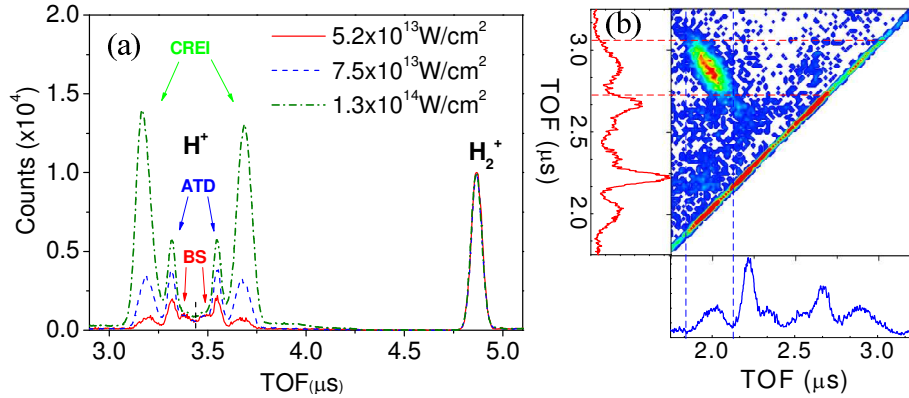


Fig. 2. (a) Time-of-flight spectra of H_2 at different driving intensities, normalized by using the H_2^+ peaks. TOF: time-of-flight, BS: bond softening, ATD: above-threshold dissociation, CREI: charge resonance enhanced ionization. (b) The photoion-photoion coincidence spectrum.

The typical time-of-flight spectrum of H_2 by our 40 fs laser pulses is shown in Fig. 2(a). The most notable peak at the right side of the spectrum is H_2^+ , while the left side spectrum corresponds to H^+ ions. The left side time-of-flight spectrum contains three groups of peaks, which are symmetric around the time-of-flight time of 3438 ns which marks the time-of-flight of H^+ with zero start velocity. The forward ions have shorter flight times than the backward flying ions. Previous works [11,13,14] have already identified these peaks, where the two-fold structure of the time-of-flight directly indicates that the H^+ ions are originated from different fragmentation channels as labeled in Fig. 2(a). The charge resonance enhanced ionization induced fragmentation channel relatively increases with respect to the bond softening and above-threshold dissociation channels as the driving intensity increases, which is consistent with the previous studies [13,14]. The Coulomb explosion induced fragmentation channel can be seen clearly by taking the corresponding photoion-photoion coincidence spectrum [15,16], as shown in Fig. 2(b). The true momentum correlation is found as a diagonal in this spectrum. Figure 2(b) shows that the charge resonance enhanced ionization events have their maximum in the diagonal line, so a correlation between the peak around 2000 and 2900 ns is identified, which corresponds to the $(H^+ + H^+)$ Coulomb explosion channel.

In our experiments, the polarization of the laser field is parallel to the spectrometer axis (z-axis), leading to a maximum ionization probability of the diatomic molecules orientating along this direction [17,18]. As shown in Fig. 3(a), a dumbbell-shaped momentum distribution along the z-axis is observed (i.e. P_z is much larger than P_x and P_y). The charge resonance enhanced ionization induced Coulomb explosion channel with fragmentation momentum of ~ 17 a.u. is clearly seen. Both momentum distributions of the Coulomb explosion induced H^+ fragments for the cases with and without software cooling are shown in Fig. 3. As the software cooling is applied, the momentum distribution become slightly sharper and narrower by removing the thermal movement of the warm molecules. Here, the small difference between of the momentum distributions when the software cooling is applied or not is due to the broad momentum bandwidth of the dissociation channel that we studied as compared to the thermal effect. For dissociation channel with narrow momentum bandwidth, the software

cooling influence will be much more visible, and is expected to be comparable to the Coltrims. The momentum resolution, depending on the position and timing resolution, can be improved by using tighter focusing condition or electrostatic lens to reduce the volume effect.

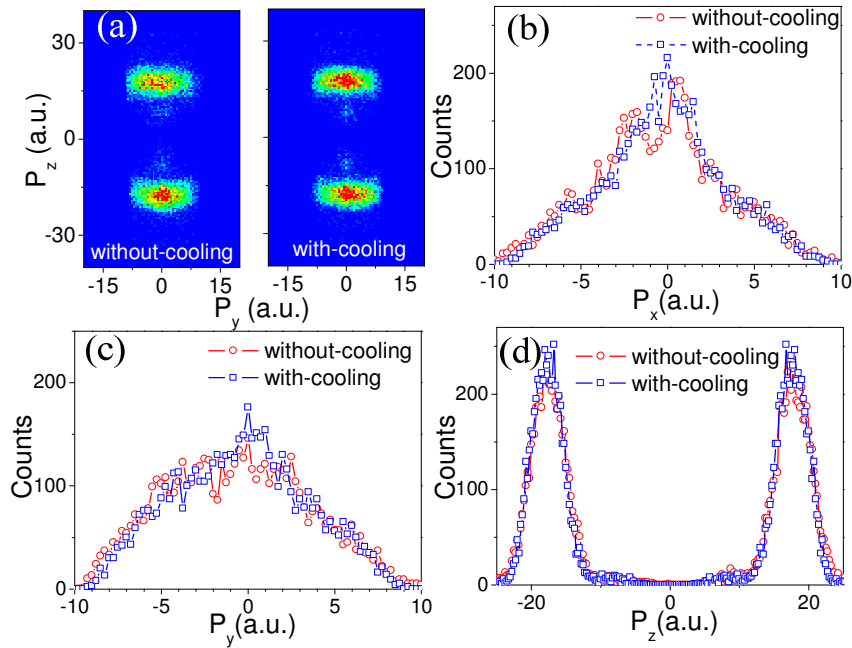


Fig. 3. The momentum distributions of the Coulomb explosion induced fragments H^+ with and without software cooling.

For charge resonance enhanced ionization based Coulomb explosion process, the kinetic energy release of the resulted fragment is determined by the number of absorbed photons n , the binding energy E_v of the particular vibrational state v , and the position R_c where the second electron is ionized, which reads as $E_{CREI} = E_{diss} + 1/R_c = (E_v + n\hbar\omega) + 1/R_c$. Figure 4(a) shows the kinetic energy distribution of the single ionization induced dissociation channel (i.e., $H_2^+ \rightarrow H^+ + H$). It was shown that [11,15,19], with photons at 800nm, the vibrational states $v \geq 5$ can dissociate through bond softening, while the states from $v=0$ to 6 require net- 2ω processes to dissociate through above-threshold dissociation. The kinetic energy release distribution of the bond softening and above-threshold dissociation induced fragments thus can be used to estimate the population probabilities of various vibrational states. As shown in Fig. 4(a), we therefore numerically fitted the measured kinetic energy release distribution by assuming Gaussian shaped distribution of each vibration state. For our experimental conditions, the bond softening and above-threshold dissociation processes are respectively dominated by the vibrational states of $v=5$ and $v=3$, while the vibrational states of $v=5$ and 6 contribute both the bond softening and above-threshold dissociation processes. The position R_c where the Coulomb explosion occurs can be further estimated from the measured kinetic energy release spectrum of the Coulomb explosion process [red-dashed curve in the inset of Fig. 4(b)]. Figure 4(b) shows the sequential ionization rate of the second electron as a function of internuclear separation. Here, an average energy of the dissociation channel (~ 0.5 eV) is used to derive the internuclear separation [19]. It was predicted that [9] there would be two internuclear separations around $R_c=7$ and 10 a.u., where the second electron is much easier to be ionized for the suppressed double-well potential. Previous experiments [6] found that it was hard to observe the enhanced ionization at $R_c=10$ a.u. since it yields a smaller kinetic energy release peak than the peak around $R_c=7$ a.u.. As shown in Fig. 4(b), besides a peak

around $R_c=6.6$ a.u., a small peak near $R_c=13.2$ a.u. is observed. This could account for the second charge resonance enhanced ionization position of $R_c=10$ a.u. as predicted in Ref. [9], and $R_c=9$ a.u. as observed in Ref. [11].

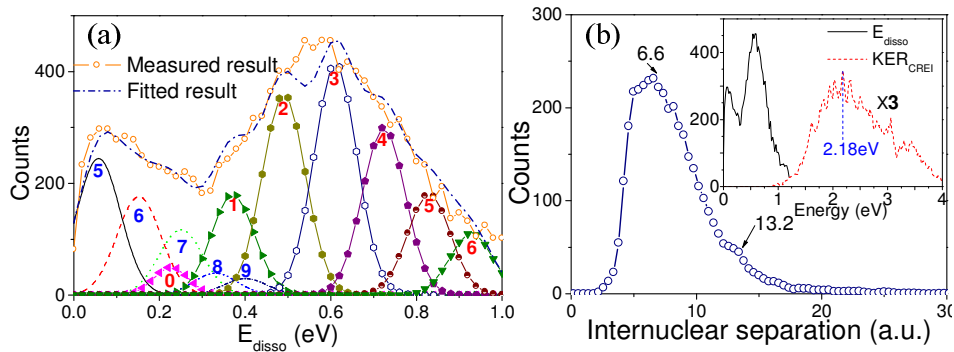


Fig. 4. (a) Measured and fitted dissociation energy of the single-ionization-induced H^+ fragmentation at a driving intensity of $7.5 \times 10^{13} \text{ W/cm}^2$. (b) The charge resonance enhanced ionization probability as a function of internuclear separation. The inset is the E_{disso} as well as the E_{CERI} spectrum of H^+ .

5. Summary

In summary, we demonstrate that the Wartrims can be used to study the fragmentation dynamics of room-temperature molecules. Our experiment distinguishes itself from previous Coltrims-experiments because warm target gas is used here with the software cooling technique to remove the thermal movement of the molecules. Taking the H_2 molecules exposed to femtosecond laser pulse at 800 nm as an example, different fragmentation channels are identified. The measured kinetic energy release spectra are used to estimate the population probabilities of the vibrational states of the H_2^+ ground state, and the second internuclear separation for charge resonance enhanced ionization around $R_c=13.2$ a.u. is observed.

Acknowledgement

This work was funded in part by National Natural Science Fund (Grants 10525416 and 10804032), National Key Project for Basic Research (Grant 2006CB806005), Projects from Shanghai Science and Technology Commission (Grant 08ZR1407100 and 09QA1402000), Program for Changjiang Scholars and Innovative Research Team in University, and Shanghai Educational Development Foundation (Grant 2008CG29). The authors thank the helpful discussions with O. Jagutzki.